8-28-2015

Development of the CRISPR/Cas9 System for Targeted Gene Disruption in Aspergillus Fumigatus

Kevin Fuller
Dartmouth College

Shan Chen
Dartmouth College

Jennifer J. Loros
Dartmouth College

Jay C. Dunlap
Dartmouth College

Recommended Citation

Fuller, Kevin; Chen, Shan; Loros, Jennifer J.; and Dunlap, Jay C., "Development of the CRISPR/Cas9 System for Targeted Gene Disruption in Aspergillus Fumigatus" (2015). *Open Dartmouth: Faculty Open Access Articles*. 811.
https://digitalcommons.dartmouth.edu/facoa/811

Development of the CRISPR/Cas9 System for Targeted Gene Disruption in *Aspergillus fumigatus*

Kevin K. Fuller,[a] Shan Chen,[a] Jennifer J. Loros,[b] Jay C. Dunlap[a]

Department of Genetics, Geisel School of Medicine at Dartmouth, Hanover, New Hampshire, USA[a]; Department of Biochemistry, Geisel School of Medicine at Dartmouth, Hanover, New Hampshire, USA[b]

Low rates of homologous recombination have broadly encumbered genetic studies in the fungal pathogen *Aspergillus fumigatus*. The CRISPR/Cas9 system of bacteria has recently been developed for targeted mutagenesis of eukaryotic genomes with high efficiency and, importantly, through a mechanism independent of homologous repair machinery. As this new technology has not been developed for use in *A. fumigatus*, we sought to test its feasibility for targeted gene disruption in this organism. As a proof of principle, we first demonstrated that CRISPR/Cas9 can indeed be used for high-efficiency (25 to 53%) targeting of the *A. fumigatus* polyketide synthase gene (*pksP*), as evidenced by the generation of colorless (albino) mutants harboring the expected genomic alteration. We further demonstrated that the constitutive expression of the Cas9 nuclease by itself is not deleterious to *A. fumigatus* growth or virulence, thus making the CRISPR system compatible with studies involved in pathogenesis. Taken together, these data demonstrate that CRISPR can be utilized for loss-of-function studies in *A. fumigatus* and has the potential to bolster the genetic toolbox for this important pathogen.

*A*spergillus fumigatus is a ubiquitous saprophytic fungus that plays an essential role in carbon and nitrogen recycling within ecosystems but is also a major cause of disease in immunocompromised individuals (1, 2). Over the past several decades, the incidence of invasive aspergillosis has risen along with the susceptible patient population, thus highlighting the need for a better understanding of virulence determinants in the fungus (3–5). The most powerful approach in this regard remains the generation and analysis of mutants. Randomized UV or insertional mutagenesis screens have been used on a limited basis to identify essential genes (6) as well as novel pigmentation (7) and drug-resistant mutants (8). However, due to the growing comparative genomic and biological data from other fungi, the major approach in recent years has by far been that of reverse genetics, involving the targeted disruption of candidate genes.

The major limitation for gene deletion in *A. fumigatus*, and indeed most filamentous fungi, has been the relatively low rates of homologous recombination, reported as lower than 5% depending on the gene (9). This is due largely to the presence of nonhomologous end joining (NHEJ) systems that preferentially promote the ectopic insertion of the targeting DNA. The high false-negative ratios among transformants, coupled with laborious and often low-yield transformation techniques (e.g., chemical transformation of protoplasts), may necessitate the screening of hundreds of transformants across multiple transformation attempts before the desired mutant is isolated. Consequently, several groups have developed *A. fumigatus* recipient strains in which the NHEJ pathway (Δ*ku70* or Δ*ku80*) is disabled, allowing homologous recombination to occur at a higher frequency among transformants (9, 10). Newer and more elegant methods, such as the hygromycin resistance split-marker approach, where fragments of a selectable marker must recombine homologously in order to confer drug resistance, further increase the probability of obtaining the desired mutant (11).

Another limiting factor for mutagenesis in *A. fumigatus* stems from the restricted number of dominant selectable markers, of which there are three predominantly employed: the hygromycin phosphotransferase gene (*hph*) for hygromycin selection, *ble* for phleomycin resistance, and *ptrA* for pyrithiamine selection. Therefore, work in wild-type (i.e., prototrophic) backgrounds permits the deletions of only three genes, which are performed in successive transformations. Several auxotrophic strains have been employed by the community, including *adeA*, *adeB*, *argB*, *niaD*, *pyrG*, *pyrE*, *sC*, and *trpC*. A limitation of using such strains, however, is the loss of virulence observed in some of the strains, e.g., *pyrG* strains (12); thus, proper isogenic controls for virulence experiments may be lacking.

Finally, the need for homologous genomic targeting may be bypassed by gene silencing with RNA interference (RNAi). Whereas this method provides an advantage of targeting multiple gene products, a complete loss of target gene expression has never been achieved in this system (13, 14).

A more recent alternative to homologous repair-based techniques is the clustered, regularly interspaced, short palindromic repeat (CRISPR) technology utilizing an RNA-guided nuclease, CRISPR-associated (Cas9) protein. CRISPR/Cas9 originates as a prokaryotic adaptive defense system against invading viruses and DNA (15, 16). Remarkably, and in just the past 2 years, the system derived from *Streptococcus pyogenes* (17) has been simplified as a genomic engineering tool in diverse eukaryotes, such as mice and

rats ([18–21]), plants ([22], [23]), and even fungi, including *Saccharomyces cerevisiae* ([24]), *Candida albicans* ([25]), *Trichoderma reesei* ([26]), and other *Aspergillus* spp. ([27]). Briefly, a synthetic single-guide RNA (gRNA), which is a fusion of CRISPR RNA (crRNA) and *trans*-activating crRNA (tracrRNA), associates with endonuclease Cas9 and guides it to a 20-nucleotide genomic target. When the genomic target is adjacent to a Cas9-specific protospacer-adjacent motif (PAM), 5′-NGG, Cas9 will induce a double-strand DNA break ([17], [28], [29]). Indel mutagenesis occurs through NHEJ in genomic targets, inducing frameshifts and resulting in nonsense mutations or otherwise nonfunctional proteins. For the CRISPR/Cas9 system in yeast it has been reported that through short NHEJ-mediated indels, there is a 469-fold increase in mutation frequency for target gene disruption after *cas9* gene induction ([24]). Moreover, the simultaneous targeting of multiple loci can be achieved by introducing multiple and unique gRNA sequences ([18], [26]).

In summary, the CRISPR/Cas9 system provides the benefits of RNAi in that it bypasses the need for homologous recombination and allows for the targeting of multiple genes in a single transformation; however, it is perhaps more attractive than RNAi in that it works at the genomic level, making gene silencing complete and stable. In this report, we demonstrate that CRISPR/Cas9 can be used for high-efficiency gene disruption in *A. fumigatus*, using the *pksP* gene (essential for melanin production) as a case study ([30], [31]). We also demonstrate that constitutive expression of Cas9 alone does not alter growth rate, development, resistance to oxidative stress, cell wall homeostasis, antifungal sensitivity, or virulence in a murine model. This, importantly, establishes that *A. fumigatus* mutants generated with CRISPR/Cas9 are compatible for pathogenesis studies. In addition, we describe an NHEJ-mediated integration of transforming DNA to the Cas9 cut site, a phenomenon that, to our knowledge, has not been described in other fungal CRISPR systems.

MATERIALS AND METHODS

Vector construction and transformation into *A. fumigatus*. All PCRs for vector construction were performed with Phusion Flash DNA polymerase (Thermo Fisher) unless otherwise noted. All primer sequences are listed in Table S1 in the supplemental material.

(i) p-*hph*-P*tef1*-*cas9*-*pksP*-gRNA for introduction into wild-type *A. fumigatus*. The hygromycin phosphotransferase (*hph*) cassette was amplified from pAN7-1 using primers 1 and 2. The P*tef1*-*cas9* cassette was amplified from p414-TEF1p-Cas9-CYC1t (Addgene plasmid 43802) with primers 3 and 4. The *pksP*-gRNA cassette was generated across three PCRs: (i) the SNR52 promoter was amplified from p426-SNR52p-gRNA.CAN1.Y-SUP4t (Addgene plasmid 43803) with primers 5 and 6, (ii) the *pksP*-gRNA was amplified from p426-SNR52p-gRNA.CAN1.Y-SUP4t using primers 7 and 8, and (iii) the SNR52 promoter and *pksP*-gRNA fragments were fused in an overlap PCR using primers 5 and 8. Finally, the *hph*, *cas9*, and *pksP*-gRNA fragments were assembled and cloned into pRS426 by homologous recombination within *S. cerevisiae* cells ([32]). Yeast clones were screened by PCR, and the desired p-*hph*-P*tef1*-*cas9*-*pksP*-gRNA was purified. The purified plasmid was used as a template for PCR using primers 1 and 8, and the resulting *hph*-*cas9*-gRNA product was introduced into Af293 protoplasts as described below.

(ii) p-*bleR*-*pksP*gRNA for introduction into *cas9*-*hph* strains. The *bleR* cassette was amplified from pBC-phleo ([33]) using primers 11 and 12. The *pksP*-gRNA cassette was generated across three PCRs: (i) the SNR52 promoter was amplified from p426-SNR52p-gRNA.CAN1.Y-SUP4t with primers 13 and 6, (ii) the *pksP*-gRNA was amplified from p426-SNR52p-gRNA.CAN1.Y-SUP4t using primers 7 and 14, and (iii) the SNR52 promoter and *pksP*-gRNA fragments were fused in an overlap PCR using

primers 13 and 14. Finally, the *bleR* and *pksP*-gRNA fragments were fused in an overlap PCR using primers 11 and 14, and the overlap product was cloned into pSC-amp/kan (Strataclone). The p-*bleR*-*pksP*-gRNA plasmid was linearized with KpnI restriction endonuclease and introduced into either the Af293 or CEA10 *cas9*-*hph* strain by chemical transformation as described below.

(iii) p-*hph*-*pksP*-gRNA for transformation into wild-type *A. fumigatus*. The *hph* cassette was amplified with primers 1 and 20. The *pksP*-gRNA cassette was generated across three PCRs: (i) the SNR52 promoter was amplified from p426-SNR52p-gRNA.CAN1.Y-SUP4t with primers 21 and 6, (ii) the *pksP*-gRNA was amplified from p426-SNR52p-gRNA.CAN1.Y-SUP4t using primers 7 and 8, and (iii) the SNR52 promoter and *pksP*-gRNA fragments were fused in an overlap PCR using primers 21 and 8. Finally, the *hph* and *pksP*-gRNA fragments were assembled and cloned into pRS426 by homologous recombination within *S. cerevisiae* cells. The resulting p-*hph*-*pksP*-gRNA plasmid was used as a template for PCR using primers 1 and 8. The resulting product was introduced into Af293 wild-type protoplasts as described below.

Chemical transformation of *A. fumigatus* protoplasts. Transformation of *A. fumigatus* protoplasts was performed as described previously ([34]) with some modification. Briefly, conidia were incubated in glucose minimal medium (GMM) (1% glucose, 10 mM ammonium tartrate, salts, pH 6.5) supplemented with 0.5% yeast extract for 10 h at 30°C. Following incubation, the cell wall of germlings was digested with 3.5 mg/ml lysing enzymes (Sigma, L1412) for 5 h at 28°C. Protoplasts were transformed with ~10 μg DNA using 60% polyethylene glycol (PEG) 3350 (Sigma-Aldrich) and plated onto GMM supplemented with 1.2 M sorbitol. Following 24 h of incubation at room temperature, plates were overlaid with top agar containing hygromycin or phleomycin and subsequently incubated at 37°C.

***A. fumigatus* strains used for this study.** The wild-type *A. fumigatus* strain Af293 was obtained from Judith C. Rhodes at the University of Cincinnati, and the wild-type CEA10 and Δ*pksP* mutant (Af293 background) were obtained from Robert A. Cramer, Jr., at Dartmouth.

For construction of the *cas9*-*hph* strains, the *hph*-*cas9* fragment was amplified from the p-*hph*-P*tef1*-*cas9*-*pksP*-gRNA plasmid (see above) using primers 9 and 10. The PCR product was then introduced into wild-type Af293 or CEA10 protoplasts by chemical transformation as described above. Integration of the *cas9* gene into transformants was initially determined by PCR of gDNA with primers 3 and 4, followed by Southern blotting (described below).

Southern blotting. The number of sites into which the *cas9* gene was integrated in Af293 or CEA10 recipient strains was analyzed by Southern blotting using the digoxigenin (DIG) system (Roche). Briefly, 40 μg of genomic DNA was digested in a BamHI and NcoI double digestion in buffer 3.1 (New England BioLabs) overnight at 37°C and then electrophoresed in a 1% Tris-acetate-EDTA (TAE) agarose gel at 50 V for 2 h. The gel was transferred onto a positively charged nylon membrane (Roche) via capillary transfer overnight in 20× SSC buffer (1× SSC is 0.15 M NaCl plus 0.015 M sodium citrate). The membrane was hybridized overnight at 42°C with 200 ng/ml of a 2.4-kb DIG probe (Roche) targeted to the *cas9* gene (see Fig. S1A in the supplemental material). The probe was stained with anti-DIG–alkaline phosphatase (AP) antibody (Roche) and visualized with chemiluminescent CDP-Star (Roche) according to the manufacturer's instructions. The membrane was exposed to a chemiluminescent X-ray film (GE Healthcare) for 1 to 2 min to visualize bands.

Western blotting. The expression of Cas9 in the *cas9*-*hph* strains was analyzed by Western blotting. Briefly, overnight 37°C liquid cultures of recipient strains were collected, lyophilized, and mechanically broken using 3.5-mm steel beads in protein extraction buffer (50 mM Tris-HCl [pH 7.5], 0.1 M EDTA, 1 mM β-mercaptoethanol) and protease inhibitor (Pierce) for 2 min. The slurry was incubated on ice for 10 min, and then the supernatant was collected after centrifugation at 4°C. The protein amount was determined by the Bradford method using protein assay dye reagent concentrate (Bio-Rad). Twenty micrograms of protein was loaded into a 3 to 8% Tris-acetate polyacrylamide gel and wet transferred to a polyvinylidene difluoride (PVDF)
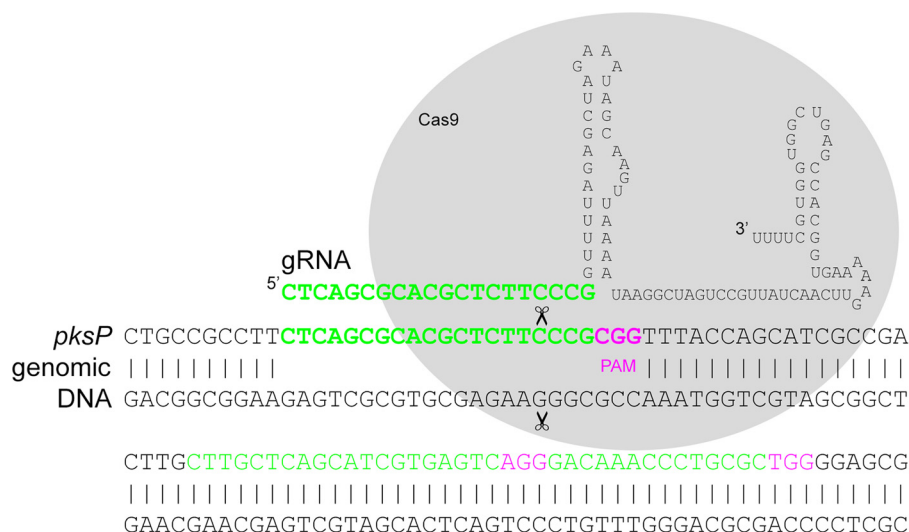
FIG 1 Diagram of the *pksP*-targeting Cas9/gRNA complex. The illustration shows the *pksP*-specific guide RNA (gRNA) used in this study associating with the Cas9 endonuclease. The locations of the protospacer-adjacent motif (PAM), Cas9 double-strand cut site (3 to 4 nucleotides upstream of the PAM site), and other candidate gRNAs within the first exon are shown (green).

membrane (Millipore). The membrane was stained with a 1:500 dilution of anti-Cas9 monoclonal antibody (Epigentek), washed, and then stained with a 1:3,000 dilution of anti-mouse IgG horseradish peroxidase (HRP)-conjugated antibody (Bio-Rad). The membrane was visualized with SuperSignal West Pico chemiluminescent substrate (Thermo Scientific) according to the manufacturer's instructions and exposed to a chemiluminescence-sensitive X-ray film (GE Healthcare) for 1 to 2 min.

Reverse transcription-PCR (RT-PCR) analysis. Conidia of the wild-type and *cas9-hph* strains were incubated in GMM (supplemented with 0.5% yeast extract) overnight at 37°C. Tissue was harvested by brief vacuum filtration and then frozen with liquid nitrogen. RNA was isolated by crushing the frozen tissue with a glass rod and processing the powder with an RNeasy kit (Qiagen). Two micrograms of RNA was used for first-strand synthesis (Superscript III; Invitrogen), and 1 μl of cDNA was used in a 20-μl PCR mixture using primers 15 and 16.

Sequencing of the target locus in transformant colonies. The coding sequence of *pksP* (Afu2g17600) was amplified from each of the strains using Phusion Flash DNA polymerase and primers 17 and 18 and then cleaned using a PCR purification kit (Qiagen). The 1.3-kb region surrounding the gRNA cut site was sequenced at the Molecular Biology Core at Dartmouth using primer 19.

Growth rate and stress resistance assays. To assess the radial growth rate, 2 μl of a 5×10^6 ml^{-1} conidial suspension of the indicated strains was point inoculated onto the center of a GMM plate. Plates were incubated for 72 h at 37°C.

For the stress tolerance assays, 2 μl of a 5×10^6 ml^{-1} conidial suspension was point inoculated onto GMM containing the indicated drug. Plates were incubated for 48 h at 37°C.

Virulence determination. All animal experiments were approved by the Institutional Animal Care and Use Committee at Dartmouth College. Groups of female CD-1 mice (Charles River Laboratories) were injected subcutaneously with 40 mg/kg of triamcinolone acetonide (Kenalog-10; Bristol-Meyers Squibb). On the following day (day 0), animals were anesthetized in an isoflurane chamber and inoculated intranasally with fungal conidia suspended in 25 μl phosphate-buffered saline (PBS); Af293 animals received 1.0×10^6 conidia, whereas CEA10 animals received 5.0×10^5 conidia. The Af293 animals (both wild type and *cas9-hph*) received a second 40-mg/kg injection on day +3. Moribund animals were euthanized by CO_2 asphyxiation. Mortality curves for the wild-type- and *cas9-hph*-infected groups were compared by the log rank test.

Quantitation of conidiation. A 120-μl portion of a 1.0×10^6 ml^{-1} conidial suspension was plated across 15-mm GMM agar plates and incubated for either two (Af293 background) or three (CEA10 background) days at 37°C. Following incubation, conidia were harvested by swabbing conidia into 10 ml of sterile water, and this was repeated three times (40 ml total). Conidial suspensions were diluted and subsequently enumerated with a hemacytometer. Three plates were analyzed per group.

RESULTS

Targeted disruption of *pksP* in wild-type *A. fumigatus* using CRISPR/Cas9. Our overall goal was to assess the feasibility of using the CRISPR/Cas9 system for targeted gene disruption in *A. fumigatus*. As a proof of principle, we chose to target the *pksP* gene (AFUA_2G17600), encoding a polyketide synthase essential in the synthesis of dihydroxynaphthalene (DHN) melanin. In contrast to wild-type *A. fumigatus* colonies, which appear green due to the production of melanized conidia, Δ*pksP* mutants appear completely white (albino) (30, 31). Accordingly, the successful disruption of *pksP* could be determined simply by the presence of albino transformants, and the overall targeting efficiency could be discerned from the phenotypic ratios.

The target gRNA sequence was designed based on criteria that had proved successful in *S. cerevisiae* (24). First, we searched for PAM sites (-NGG) that existed within an exon and approximately 100 to 200 nucleotides downstream of the *pksP* translational start. The 13-nucleotide sequence directly upstream of each PAM site (i.e., the seed sequence) was used in a BLAST analysis against the *A. fumigatus* Af293 genome; those that lacked complete identity to another locus were considered candidate gRNA targets. Three sites emerged based on these criteria, the most ATG proximal of which was selected for our studies (Fig. 1).

We first generated a vector that, following random integration into the genome, would allow for *pksP* targeting in wild-type *A. fumigatus* (Fig. 2A). The construct consisted of three components: (i) P*tef1-cas9*, in which the *cas9* nuclease gene, used previously in *S. cerevisiae* (codon optimized for use in human cells), is driven by
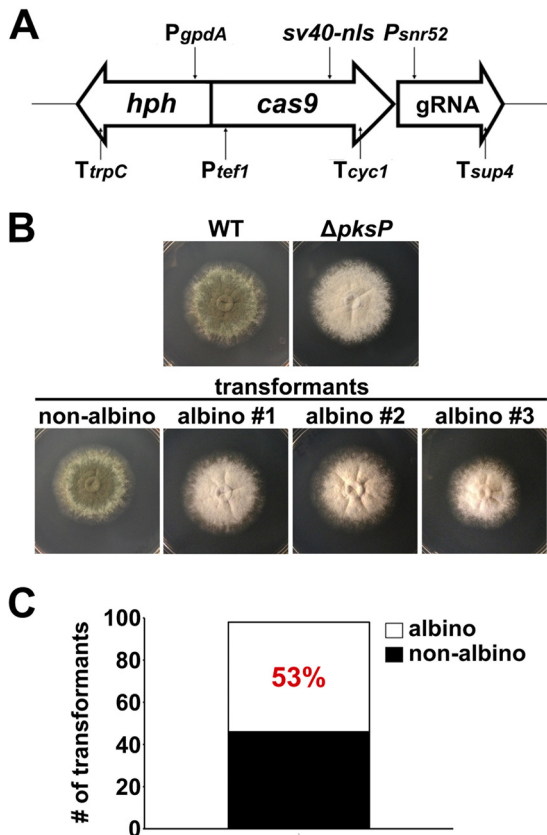
FIG 2 Disruption of *pksP* using CRISPR/Cas. (A) Scheme of the transformation construct used for transformation into Af293 protoplasts. Transcriptional promoter (P) and terminator (T) elements are noted. (B) Hygromycin-resistant transformants were incubated on GMM to assess their pigmentation phenotype. Representative transformants are shown. Albino colonies resemble the Δ*pksP* control; nonalbino colonies resemble the wild type. (C) Phenotypic ratios of the transformants.

the *tef1* promoter; (ii) *pksP*-gRNA, consisting of the above-described *pksP* target sequence fused with the structural gRNA element; and (iii) the hygromycin phosphotransferase gene (*hph*) for the positive selection of transformants. Following the fusion and cloning of the three cassettes via yeast recombination, the *hph-cas9*-gRNA insert was PCR amplified and introduced into *A. fumigatus* (strain Af293) protoplasts by chemical transformation. Two independent transformations yielded a total of 98 hygromycin-resistant colonies, which were subcultured onto GMM plates and incubated for 72 h at 37°C to assess their phenotype. Remarkably, 52 transformants (53%) resembled the Δ*pksP* control strain, whereas the remaining colonies were indistinguishable from the wild type (Fig. 2B and C), indicating that the CRISPR/Cas9 system can indeed function in *A. fumigatus* with high efficiency.

Because the gRNA portion *hph-cas9*-gRNA cassette contains homology to the genomic target, albeit across a small region (20 bp), we wanted to exclude the possibility that *pksP* disruption was due to a homologous recombination event. Accordingly, constructs containing the *pksP*-gRNA alone (gRNA-*hph*) or the *cas9* gene alone (*cas9-hph*) were generated and introduced into Af293 wild-type protoplasts. Whereas albino transformants were generated from the *hph-cas9*-gRNA construct, all hygromycin-resistant colonies derived from the gRNA-*hph* or the *cas9-hph* transforma-

tions resembled the wild type (see Fig. S1 in the supplemental material). This suggested that both the *cas9* gene and the *pksP*-gRNA are essential components for *pksP* targeting in our system and that the contribution of homologous recombination alone is negligible.

Effect of constitutive *cas9* expression on *A. fumigatus* growth and virulence. If mutants generated with the CRISPR system are to be useful for pathogenesis studies, it is imperative that expression of the *cas9* nuclease itself is not deleterious with respect to *A. fumigatus* growth or virulence. We sought to test this by generating strains that constitutively express *cas9* without the presence of a targeting gRNA. To do so, the P*tef1-cas9* cassette (described above) was fused with the *hph* marker, and the resulting construct (the same used in the control transformation described above) was introduced into the two most commonly employed *A. fumigatus* strains, Af293 and CEA10 (Fig. 3A). The integration of *cas9* into the genome of hygromycin-resistant colonies was first tested by PCR (data not shown) and then confirmed by Southern blotting (see Fig. S2A in the supplemental material). The expression of *cas9* was subsequently confirmed by both Western blot (see Fig. S2B in the supplemental material) and RT-PCR (Fig. 3A) analyses. The colonial appearance of all *cas9*-expressing transformants (called *cas9-hph*) was identical to that of the respective Af293 or CEA10 recipient strain. A single isolate in either background, chosen on the basis of fewest *cas9* integrations by Southern blotting, was chosen for further phenotypic analysis and use.

We first tested growth rate by spotting conidia of each strain onto GMM plates and incubating for 72 h at 37°C. As shown in Fig. 3B, the colony diameters of the *cas9-hph* strains were indistinguishable from those of their respective wild-type controls at each time point, indicating that growth rate was unaffected by *cas9* expression. The amount of conidia produced by the *cas9-hph* strains was also identical to that of the wild type, suggesting that asexual development was also unaffected (see Fig. S3 in the supplemental material).

To broadly assess the impact of *cas9* expression on stress resistance and cellular homeostasis, we tested the sensitivity of the *cas9-hph* strains against a panel of stressing agents. Included in the analysis were hydrogen peroxide, which induces oxidative stress through the induction of hydroxyl radicals (35), Congo red, which perturbs the cell wall by binding polysaccharide fibrils (36), and fungin (a polyene) and voriconazole, which affect cell membrane homeostasis either by binding ergosterol in the membrane or by inhibiting its synthesis, respectively (37). In all cases, the sensitivity of the *cas9-hph* strain was identical to that of its respective wild-type strain, suggesting that homeostasis in response to these stresses is not affected by the expression of *cas9* (Fig. 3C).

Finally, the virulence of the strains was tested in a murine model of invasive aspergillosis. Briefly, groups of CD-1 outbred mice were immunosuppressed with the synthetic corticosteroid triamcinolone acetonide and then subsequently inoculated intranasally with the indicated strains. Whereas the animal survival curves are different in the Af293 and CEA10 backgrounds, the *cas9-hph* strains were statistically indistinguishable from their respective wild-type controls (Fig. 3D).

In summary, constitutive expression of the *cas9* endonuclease does not alter growth, development, stress resistance, and, importantly, virulence in either the Af293 or CEA10 background of *A. fumigatus* under the tested conditions.

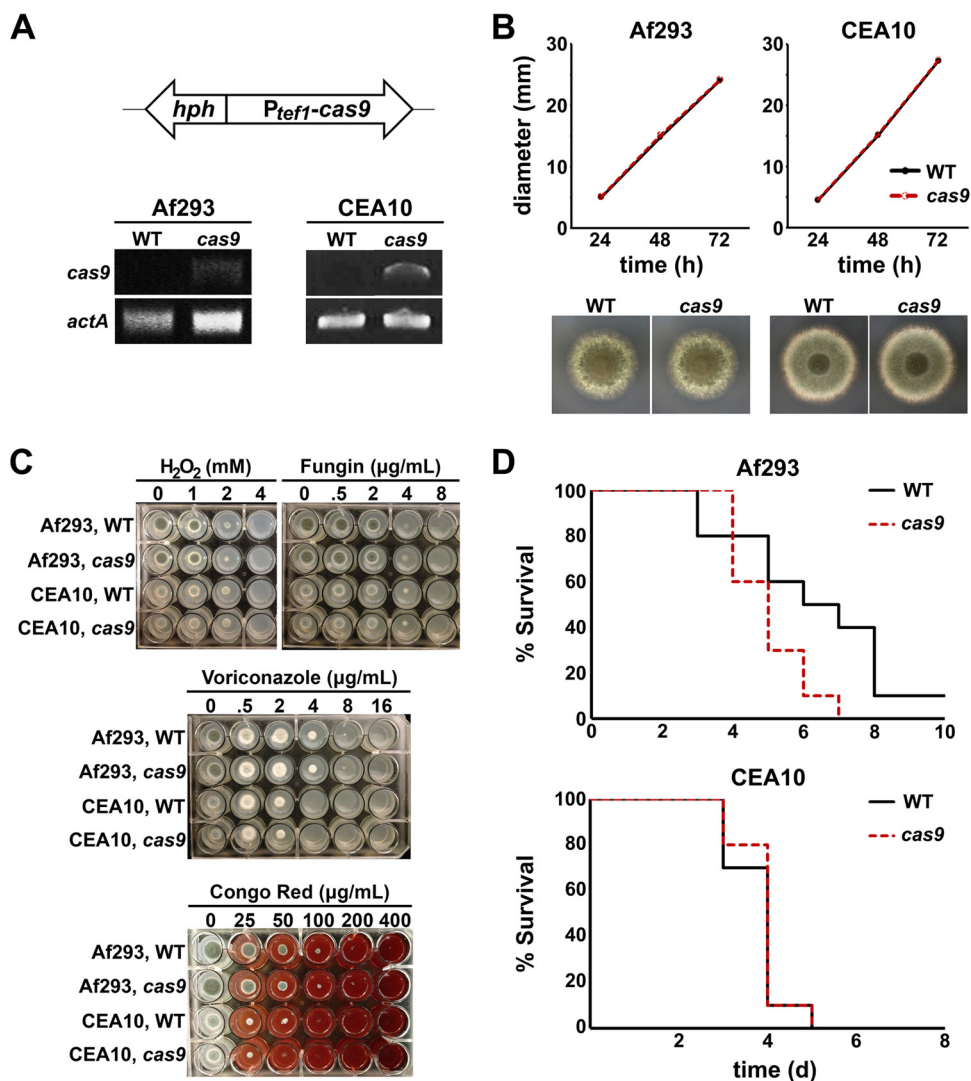**The *cas9-hph* strains as recipients for gRNA transformation.**

FIG 3 Generation and analysis of constitutive *cas9*-expressing strains. (A) Top, scheme of the construct used for transformation into Af293 or CEA10 wild-type protoplasts. Bottom, RT-PCR analysis confirming *cas9* expression in the transformants. (B) Growth rate analysis. Conidia of the indicated strains were point inoculated on GMM and incubated for 72 h at 37°C. Pictures, shown below the respective growth curve, were taken following the 72 h of incubation. (C) Stress sensitivity. Conidia were point inoculated onto GMM plates containing increasing concentrations of the indicated drugs and incubated for 48 h at 37°C. (D) Virulence. Groups of 10 CD-1 mice were immunosuppressed with triamcinolone acetonide and inoculated intranasally with the indicated strains.

We next assessed whether the *cas9-hph* strains could serve as recipients for a separate gRNA transformation. A plasmid that contained both the *pksP*-gRNA (described above) and the *bleR* cassette (bleomycin/phleomycin resistance) as a selectable marker was constructed (Fig. 4). Linearized plasmid was introduced into either the Af293 or CEA10 *cas9-hph* strain by chemical transformation, and the phenotypes of the phleomycin-resistant colonies were analyzed following incubation on GMM. In the Af293 background, 19 out of 41 (46.3%) phleomycin-resistant colonies displayed the albino phenotype, whereas 16 out of 63 (25.4%) were albino in the CEA10 background (Fig. 4). Cumulatively, these data suggest that *pksP* targeting via CRISPR/Cas is efficient in both the Af293 and CEA10 backgrounds. Moreover, the *cas9-hph* strains can be used as recipient strains for downstream gRNA transformation and in this way may serve as universal strains for CRISPR-mediated mutagenesis.

Genotypic analysis of the *pksP* locus in both albino and non-albino transformants. The Cas9/gRNA complex is known to induce double-strand breaks at the gRNA target sequence, which are then resolved through error-prone NHEJ in the absence of a homologous sequence (24). To determine if the albino mutants obtained in our experiments could be attributed to a similar mechanism, primers spanning the 5′ end of the *pksP* coding sequence were used to generate products (expected size, 1.5 kb), which were then subjected to Sanger sequencing. The Af293 wild-type and *cas9-hph* recipient strains were analyzed as controls, and both were identical to the Af293 genomic reference at the *pksP* locus (Fig. 5).

Two of the albino transformants in our analysis yielded a PCR product of the expected size, the sequencing of which revealed that either a single nucleotide insertion or deletion had occurred three base pairs upstream of the targeted PAM site (Fig. 5, transformants 1 and 2). An *in silico* translation of the mutant sequences
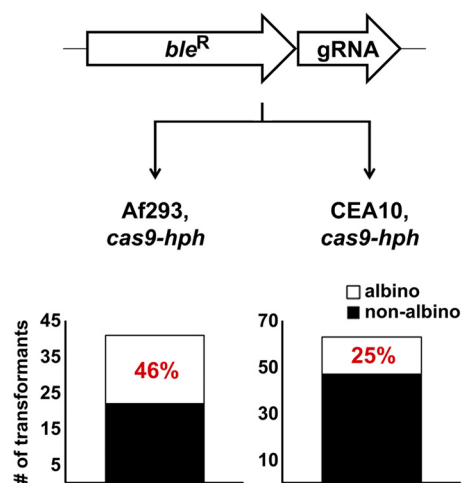
FIG 4 *pksP* targeting in *cas9-hph* recipient strains. A plasmid containing the *pksP* gRNA sequence and the bleomycin resistance gene (*ble*R) was constructed and introduced into Af293 and CEA10 *cas9-hph* recipient protoplasts. Phleomycin-resistant colonies were incubated on GMM, and the proportion of albino colonies was determined.

predicted a frameshift that would ultimately lead to a premature translational stop within 14 or 25 amino acids of the insertion or deletion, respectively (data not shown). Thus, these single nucleotide indels are consistent with the CRISPR-mediated mutations described in other systems (24).

Surprisingly, most albino colonies yielded amplicons that were of a higher molecular weight than the 1.5 kb band of wild-type, indicating perhaps that larger insertions had taken place. For the single-construct transformation into wild-type, sequencing of the amplicons indeed revealed that a portion of the transforming PCR fragment had integrated at the expected Cas9 cut site. More completely, the insertions included the 3′ end of the PCR fragment, extending variably into the structural gRNA sequence (Fig. 5, transformants 3 and 4). Because non-integrated (episomal) DNA is typically degraded in *A. fumigatus*, these data suggested that both *cas9* and the *pksP*-gRNA were rapidly expressed within the protoplasts, allowing for the NHEJ machinery to integrate part of the introduced DNA at the Cas9-mediated double-strand break.

Similarly for the transformation of the *cas9-hph* recipient strains (described in Fig. 4), four out of eight albino colonies yielded products of up to 6.5 kb larger than the expected size, suggesting that the entire linearized plasmid had been inserted into the *pksP* locus (see Fig. S4 in the supplemental material). This was confirmed, as sequencing of the high-molecular-weight bands (~8 kb) all revealed plasmid integration at the Cas9 cut site (data not shown).

We also analyzed several of the nonalbino transformants, and all yielded sequences that were identical to the wild-type reference (see Fig. S5 in the supplemental material). This suggested that the nonalbino phenotype is most likely due to a lack of targeting at the *pksP* locus, rather than an insertion/deletion that yielded no functional alteration to PksP (e.g., a single amino acid insertion).

Taken together, these data indicate that the albino phenotypes observed in our transformants were due to the expected Cas9-mediated cutting at the gRNA targeting sequence. The specific NHEJ-mediated events at the cut site varied, however, ranging

from the single-nucleotide insertion/deletions, as observed in other systems, to large insertions of transforming DNA constructs.

DISCUSSION

Gene replacement through homologous recombination can be improved by several approaches in *A. fumigatus*. First, Krappman et al. showed that by simply increasing the size of homologous flanks in the transforming construct (directed toward *abr2*), targeting efficiency could be increased from 0% (0.1-kb flanks) to 10% (1 kb) to 22% (2 kb) (10). Though targeting could presumably be increased with even larger flanking regions, the cloning efficiency becomes the limiting factor; therefore, standard protocols typically involve flanking regions of approximately 1 kb on either side of the target gene. The second approach involves introduction of DNA into mutant strains of *A. fumigatus* that are deficient in an essential component of the NHEJ pathway. For example, in the same study, the replacement of *abr2* with 0.1-kb flanks was increased to 75%, and with 2-kb flanks it was increased to 95% in a Δ*akuA* (*ku70*) mutant (10). Similarly, da Silva Ferreira et al. demonstrated that *pksP* targeting could be increased from 3% in a wild-type background to 85% in a Δ*akuB* (ku80) strain (9). Finally, *Agrobacterium tumefaciens*-mediated transformation (ATMT) of *A. fumigatus* conidia has been found to yield recombination rates of 35 to 66%, depending on the gene (38, 39).

Unlike all of the above-mentioned strategies, the CRISPR/Cas9 system bypasses the need for homologous recombination altogether, as the Cas9 nuclease is directed to its target through association with a short gRNA. In this study, we have demonstrated the utility of this system in *A. fumigatus* by disrupting the *pksP* gene with an efficiency of 25 to 53%. We propose that the system functions in *A. fumigatus* as it does in other organisms, based on two lines of evidence: (i) mutant phenotypes were observed only upon introduction of both the *cas9* gene and the gRNA, and (ii) *pksP* disruption occurred at the expected Cas9 cut site in all albino mutants tested. What is perhaps unique to our data, however, is the finding that the transforming DNA can be integrated at the Cas9 cut site, presumably through the NHEJ pathway. Indeed, this phenomenon has recently been described in a mammalian cell CRISPR system (40). However, to our knowledge, this is the first report of such construct integrations among fungal CRISPRs. Why such a mechanism might dominate (>50% of albino transformants tested) in *A. fumigatus*, but not other fungi, remains unclear.

Importantly, we have demonstrated that the CRISPR/Cas9 system works in two commonly employed strains of *A. fumigatus*, Af293 and CEA10. Although we did find different targeting ratios in the two backgrounds in our experiment (46.3% for Af293 and 25.4% for CEA10), we cannot yet state whether these differences would hold up across multiple transformations or across different loci. Nevertheless, the ability to introduce CRISPR/Cas9 constructs into any *A. fumigatus* background represents a distinct advantage of the system. In contrast, although targeting rates may be higher in NHEJ mutants (up to 95%), researchers are confined to work with strains in which *akuA/akuB* mutations have been generated.

The expression of heterologous enzymes has been known to alter fungal physiology in unpredictable ways. In the dimorphic fungal pathogen *Histoplasma capsulatum*, for example, the expression of the *hph* selectable marker does not affect growth or development but remarkably enhances virulence. This influence of
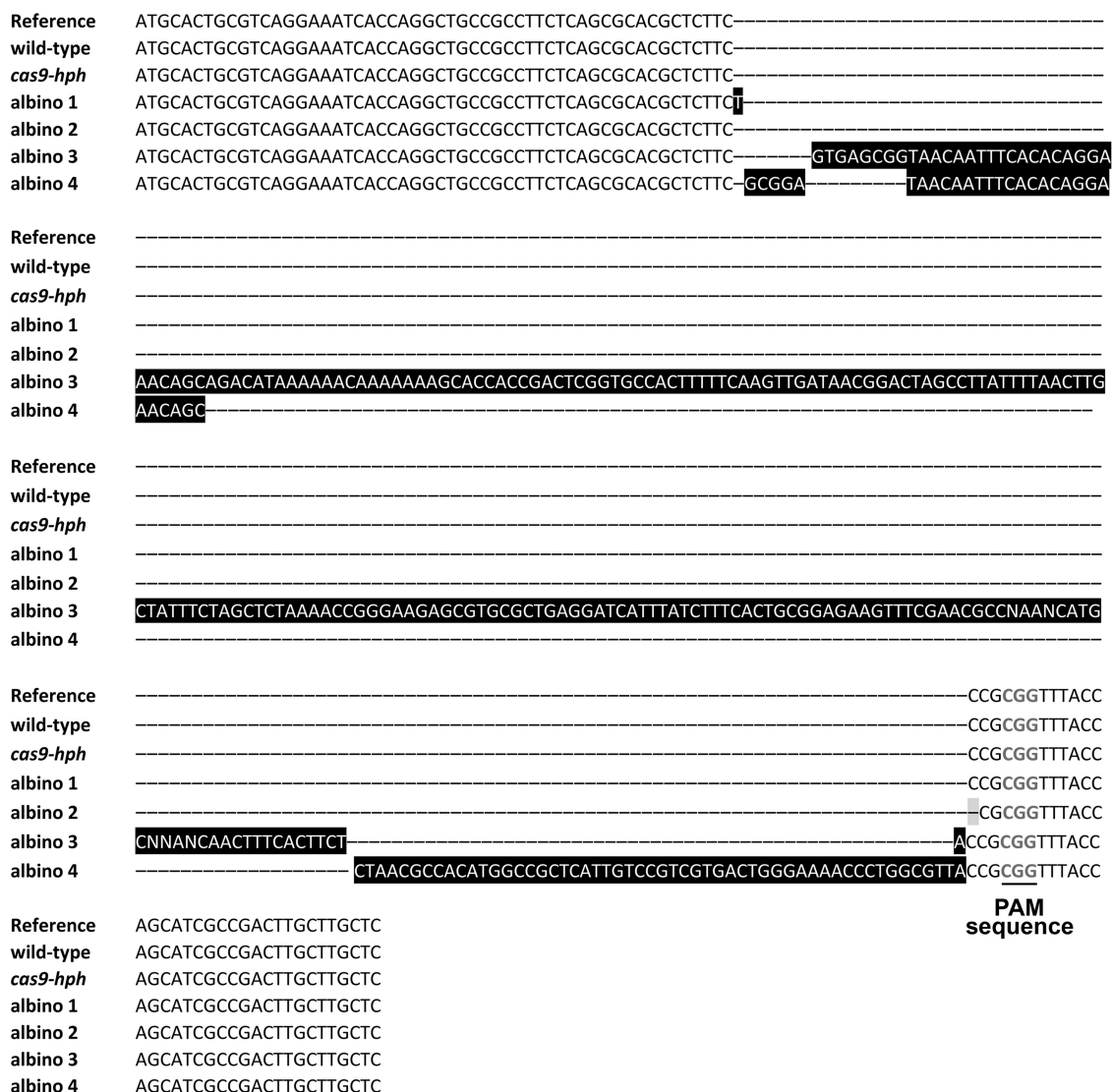
```
Reference    ATGCACTGCGTCAGGAAATCACCAGGCTGCCGCCTTCTCAGCGCACGCTCTTC————————————————————————————
wild-type    ATGCACTGCGTCAGGAAATCACCAGGCTGCCGCCTTCTCAGCGCACGCTCTTC————————————————————————————
cas9-hph     ATGCACTGCGTCAGGAAATCACCAGGCTGCCGCCTTCTCAGCGCACGCTCTTC————————————————————————————
albino 1     ATGCACTGCGTCAGGAAATCACCAGGCTGCCGCCTTCTCAGCGCACGCTCTTCT———————————————————————————
albino 2     ATGCACTGCGTCAGGAAATCACCAGGCTGCCGCCTTCTCAGCGCACGCTCTTC————————————————————————————
albino 3     ATGCACTGCGTCAGGAAATCACCAGGCTGCCGCCTTCTCAGCGCACGCTCTTC————GTGAGCGGTAACAATTTCACACAGGA
albino 4     ATGCACTGCGTCAGGAAATCACCAGGCTGCCGCCTTCTCAGCGCACGCTCTTC—GCGGA—————————TAACAATTTCACACAGGA

Reference    ——————————————————————————————————————————————————————————————————————————————————
wild-type    ——————————————————————————————————————————————————————————————————————————————————
cas9-hph     ——————————————————————————————————————————————————————————————————————————————————
albino 1     ——————————————————————————————————————————————————————————————————————————————————
albino 2     ——————————————————————————————————————————————————————————————————————————————————
albino 3     AACAGCAGACATAAAAAACAAAAAAAGCACCACCGACTCGGTGCCACTTTTTCAAGTTGATAACGGACTAGCCTTATTTTAACTTG
albino 4     AACAGC——————————————————————————————————————————————————————————————————————————————

Reference    ——————————————————————————————————————————————————————————————————————————————————
wild-type    ——————————————————————————————————————————————————————————————————————————————————
cas9-hph     ——————————————————————————————————————————————————————————————————————————————————
albino 1     ——————————————————————————————————————————————————————————————————————————————————
albino 2     ——————————————————————————————————————————————————————————————————————————————————
albino 3     CTATTTCTAGCTCTAAAACCGGGAAGAGCGTGCGCTGAGGATCATTTATCTTTCACTGCGGAGAAGTTTCGAACGCCNAANCATG
albino 4     ——————————————————————————————————————————————————————————————————————————————————

Reference    ——————————————————————————————————————————————————————————————————CCGCGGTTTACC
wild-type    ——————————————————————————————————————————————————————————————————CCGCGGTTTACC
cas9-hph     ——————————————————————————————————————————————————————————————————CCGCGGTTTACC
albino 1     ——————————————————————————————————————————————————————————————————CCGCGGTTTACC
albino 2     —————————————————————————————————————————————————————————————————— CGCGGTTTACC
albino 3     CNNANCAACTTTCACTTCT——————————————————————————————————————————————ACCGCGGTTTACC
albino 4     ————————————————————CTAACGCCACATGGCCGCTCATTGTCCGTCGTGACTGGGAAAACCCTGGCGTTACCGCGGTTTACC
                                                                                    PAM
                                                                                 sequence

Reference    AGCATCGCCGACTTGCTTGCTC
wild-type    AGCATCGCCGACTTGCTTGCTC
cas9-hph     AGCATCGCCGACTTGCTTGCTC
albino 1     AGCATCGCCGACTTGCTTGCTC
albino 2     AGCATCGCCGACTTGCTTGCTC
albino 3     AGCATCGCCGACTTGCTTGCTC
albino 4     AGCATCGCCGACTTGCTTGCTC
```

FIG 5 Sequence alignment of the *pksP* locus of albino transformants. Black-highlighted letters are used to depict nucleotide insertions at the cut site; gray-highlighted letters depict nucleotide deletions. PAM, protospacer-adjacent motif.

HPH on virulence is dependent upon its phosphotransferase activity, although the exact mechanism is unknown (41). Accordingly, we addressed concerns regarding the impact of the Cas9 nuclease on *A. fumigatus* by generating strains that constitutively express the *cas9* gene. Importantly, we report that the *cas9-hph* strains are identical to their wild-type controls with respect to all tested phenotypes, including virulence in an immunosuppressed murine model. Thus, growth- and pathogenesis-related phenotypes associated with CRISPR/Cas-generated mutants can likely be attributed to the gene under study rather than to unknown effects of the *cas9* transgene. We propose that the *cas9-hph* strains we have generated could be important community resources for all downstream CRISPR-based experiments for two reasons: (i) the large *cas9* cassette would not have to be cloned into the transformation constructs, thereby making gRNA construction more efficient and high throughput, and (ii) a strain that expresses *cas9* would serve as a more appropriate reference strain (i.e., control) than the standard wild type.

In summary, we have demonstrated that CRISPR/Cas9 can be developed as a tool for high-efficiency gene disruption in *A. fumigatus*. The further development of this technology (i.e., multigene targeting and recyclable cassettes for the reuse of selectable markers) is under way and holds significant potential for advancing the state of genetic research in this organism and, consequently, an understanding of its pathogenesis.

REFERENCES

1. **Rhodes JC.** 2006. *Aspergillus fumigatus*: growth and virulence. Med Mycol **44**(Suppl 1):S77–S81.
2. **Askew DS.** 2008. *Aspergillus fumigatus*: virulence genes in a street-smart mold. Curr Opin Microbiol **11**:331–337. http://dx.doi.org/10.1016/j.mib.2008.05.009.
3. **Upton A, Kirby KA, Carpenter P, Boeckh M, Marr KA.** 2007. Invasive aspergillosis following hematopoietic cell transplantation: outcomes and prognostic factors associated with mortality. Clin Infect Dis **44**:531–540. http://dx.doi.org/10.1086/510592.
4. **Segal BH.** 2009. Aspergillosis. N Engl J Med **360**:1870–1884. http://dx.doi.org/10.1056/NEJMra0808853.
5. **Singh N, Paterson DL.** 2005. *Aspergillus* infections in transplant recipients. Clin Microbiol Rev **18**:44–69. http://dx.doi.org/10.1128/CMR.18.1.44-69.2005.
6. **Firon A, Villalba F, Beffa R, d'Enfert C.** 2003. Identification of essential genes in the human fungal pathogen *Aspergillus fumigatus* by transposon mutagenesis. Eukaryot Cell **2**:247–255. http://dx.doi.org/10.1128/EC.2.2.247-255.2003.
7. **Jackson J, Higgins L, Lin X.** 2009. Conidiation color mutants of *Aspergillus fumigatus* are highly pathogenic to the heterologous insect host *Galleria mellonella*. PLoS One **4**:e4224. http://dx.doi.org/10.1371/journal.pone.0004224.
8. **Manavathu EK, Alangaden GJ, Chandrasekar PH.** 1998. In-vitro isolation and antifungal susceptibility of amphotericin B-resistant mutants of *Aspergillus fumigatus*. J Antimicrob Chemother **41**:615–619. http://dx.doi.org/10.1093/jac/41.6.615.
9. **da Silva Ferreira ME, Kress MRVZ, Savoldi M, Goldman MHS, Härtl A, Heinekamp T, Brakhage A, Goldman GH.** 2006. The *akuBKU80* mutant deficient for nonhomologous end joining is a powerful tool for analyzing pathogenicity in *Aspergillus fumigatus*. Eukaryot Cell **5**:207–211. http://dx.doi.org/10.1128/EC.5.1.207-211.2006.
10. **Krappmann S, Sasse C, Braus GH.** 2006. Gene targeting in *Aspergillus fumigatus* by homologous recombination is facilitated in a nonhomologous end-joining-deficient genetic background. Eukaryot Cell **5**:212–215. http://dx.doi.org/10.1128/EC.5.1.212-215.2006.
11. **Gravelat F, Askew D, Sheppard D.** 2012. Targeted gene deletion in *Aspergillus fumigatus* using the hygromycin-resistance split-marker approach. Methods Mol Biol **845**:119–130. http://dx.doi.org/10.1007/978-1-61779-539-8_8.
12. **D'Enfert C, Diaquin M, Delit A, Wuscher N, Debeaupuis JP, Huerre M, Latge JP.** 1996. Attenuated virulence of uridine-uracil auxotrophs of *Aspergillus fumigatus*. Infect Immun **64**:4401–4405.
13. **Mouyna I, Henry C, Doering T, Latgé J.** 2004. Gene silencing with RNA interference in the human pathogenic fungus *Aspergillus fumigatus*. FEMS Microbiol Lett **15**:317–324.
14. **Henry C, Mouyna I, Latgé J.** 2007. Testing the efficacy of RNA interference constructs in *Aspergillus fumigatus*. Curr Genet **51**:277–284. http://dx.doi.org/10.1007/s00294-007-0119-0.
15. **Horvath P, Barrangou R.** 2010. CRISPR/Cas, the immunes system of Bacteria and Archaea. Science **327**:167–170. http://dx.doi.org/10.1126/science.1179555.
16. **Wiedenheft B, Sternberg SH, Doudna JA.** 2012. RNA-guided genetic silencing systems in bacteria and archaea. Nature **482**:331–338. http://dx.doi.org/10.1038/nature10886.
17. **Jinek M, Chylinski K, Fonfara I, Hauer M, Doudna JA, Charpentier E.** 2012. A programmable dual-RNA–guided DNA endonuclease in adaptive bacterial immunity. Science **337**:816–821. http://dx.doi.org/10.1126/science.1225829.
18. **Cong L, Ran FA, Cox D, Lin S, Barretto R, Habib N, Hsu PD, Wu X, Jiang W, Marraffini LA, Zhang F.** 2013. Multiplex genome engineering using CRISPR/Cas systems. Science **339**:819–823. http://dx.doi.org/10.1126/science.1231143.
19. **Wang H, Yang H, Shivalila C, Dawlaty MM, Cheng A, Zhang F, Jaenisch R.** 2013. One-step generation of mice carrying mutations in multiple genes by CRISPR/Cas-mediated genome engineering. Cell **153**:910–918. http://dx.doi.org/10.1016/j.cell.2013.04.025.
20. **Shen B, Zhang J, Wu H, Wang J, Ma K, Li Z, Zhang X, Zhang P, Huang X.** 2013. Generation of gene-modified mice via Cas9/RNA-mediated gene targeting. Cell Res **23**:720–723. http://dx.doi.org/10.1038/cr.2013.46.
21. **Li D, Qiu Z, Shao Y, Chen Y, Guan Y, Liu M, Li Y, Gao N, Wang L, Lu**

X, Zhao Y, Liu M. 2013. Heritable gene targeting in the mouse and rat using a CRISPR-Cas system. Nat Biotechnol **31**:681–683. http://dx.doi.org/10.1038/nbt.2661.
22. **Jiang W, Zhou H, Bi H, Fromm M, Yang B, Weeks DP.** 2013. Demonstration of CRISPR/Cas9/sgRNA-mediated targeted gene modification in Arabidopsis, tobacco, sorghum and rice. Nucleic Acids Res **41**:e188–e188. http://dx.doi.org/10.1093/nar/gkt780.
23. **Shan Q, Wang Y, Li J, Zhang Y, Chen K, Liang Z, Zhang K, Liu J, Xi JJ, Qiu JL, Gao C.** 2013. Targeted genome modification of crop plants using a CRISPR-Cas system. Nat Biotechnol **31**:686–688. http://dx.doi.org/10.1038/nbt.2650.
24. **DiCarlo JE, Norville JE, Mali P, Rios X, Aach J, Church GM.** 2013. Genome engineering in *Saccharomyces cerevisiae* using CRISPR-Cas systems. Nucleic Acids Res **41**:4336–4343. http://dx.doi.org/10.1093/nar/gkt135.
25. **Vyas VK, Barrasa MI, Fink GR.** 2015. A *Candida albicans* CRISPR system permits genetic engineering of essential genes and gene families. Sci Adv **1**:e1500248. http://dx.doi.org/10.1126/sciadv.1500248.
26. **Rui L, Chen L, Jiang Y, Zhou Z, Zou G.** 2015. Efficient genome editing in filamentous fungus *Trichoderma reesei* using the CRISPR/Cas9 system. Cell Discovery **1**:15007. http://dx.doi.org/10.1038/celldisc.2015.7.
27. **Nødvig CS, Nielsen JB, Kogle ME, Mortensen UH.** 2015. A CRISPR-Cas9 system for genetic engineering of filamentous fungi. PLoS One **10**:e0133085. http://dx.doi.org/10.1371/journal.pone.0133085.
28. **Jiang W, Bikard D, Cox D, Zhang F, Marraffini LA.** 2013. RNA-guided editing of bacterial genomes using CRISPR-Cas systems. Nat Biotechnol **31**:233–239. http://dx.doi.org/10.1038/nbt.2508.
29. **Pattanayak V, Lin S, Guilinger JP, Ma E, Doudna JA, Liu DR.** 2013. High-throughput profiling of off-target DNA cleavage reveals RNA-programmed Cas9 nuclease specificity. Nat Biotechnol **31**:839–843. http://dx.doi.org/10.1038/nbt.2673.
30. **Langfelder K, Jahn B, Gehringer H, Schmidt A, Wanner G, Brakhage AA.** 1998. Identification of a polyketide synthase gene (*pksP*) of *Aspergillus fumigatus* involved in conidial pigment biosynthesis and virulence. Med Microbiol Immunol **187**:79–89. http://dx.doi.org/10.1007/s004300050077.
31. **Tsai HF, Chang YC, Washburn RG, Wheeler MH, Kwon-Chung KJ.** 1998. The developmentally regulated *alb1* gene of *Aspergillus fumigatus*: its role in modulation of conidial morphology and virulence. J Bacteriol **180**:3031–3038.
32. **Oldenburg KR, Vo KT, Michaelis S, Paddon C.** 1997. Recombination-mediated PCR-directed plasmid construction in vivo in yeast. Nucleic Acids Res **25**:451–452. http://dx.doi.org/10.1093/nar/25.2.451.
33. **Silar P.** 1995. Two new easy to use vectors for transformations. Fungal Genet News Lett **42**:73.
34. **Yelton MM, Hamer JE, Timberlake WE.** 1984. Transformation of Aspergillus nidulans by using a *trpC* plasmid **81**:1470–1474.
35. **Thön M, Al-Abdallah Q, Hortschansky P, Brakhage AA.** 2007. The thioredoxin system of the filamentous fungus *Aspergillus nidulans*: impact on development and oxidative stress response. J Biol Chem **282**:27259–27269. http://dx.doi.org/10.1074/jbc.M704298200.
36. **Ram AF, Klis FM.** 2006. Identification of fungal cell wall mutants using susceptibility assays based on Calcofluor white and Congo red. Nat Protoc **1**:2253–2256. http://dx.doi.org/10.1038/nprot.2006.397.
37. **Ghannoum MA, Rice LB.** 1999. Antifungal agents: mode of action, mechanisms of resistance, and correlation of these mechanisms with bacterial resistance. Clin Microbiol Rev **12**:501–517.
38. **Sugui JA, Chang YC, Kwon-Chung KJ.** 2005. *Agrobacterium tumefaciens*-mediated transformation of *Aspergillus fumigatus*: an efficient tool for insertional mutagenesis and targeted gene disruption. Appl Environ Microbiol **71**:1798–1802. http://dx.doi.org/10.1128/AEM.71.4.1798-1802.2005.
39. **Qiao JJ, Liu W, Ma Y, Wan Z, Li RY.** 2008. *Agrobacterium tumefaciens*-mediated transformation of uracil auxotroph *Aspergillus fumigatus* is an efficient method for target gene knockout. Beijing Da Xue Xue Bao **40**:330–333.
40. **Bachu R, Bergareche I, Chasin LA.** 2015. CRISPR-Cas targeted plasmid integration into mammalian cells via non-homologous end joining. Biotechnol Bioeng **112**:2154–2162. http://dx.doi.org/10.1002/bit.25629.
41. **Smulian AG, Gibbons RS, Demland JA, Spaulding DT, Deepe GS, Jr.** 2007. Expression of hygromycin phosphotransferase alters virulence of *Histoplasma capsulatum*. Eukaryot Cell **6**:2066–2071. http://dx.doi.org/10.1128/EC.00139-07.